Inelastic Alpha Scattering and Associated Gamma Radiation. II

DAVID R. INGLIS
*Argonne National Laboratory, Argonne, Illinois**
(Received 11 October 1965)

The rotational excitation of a deformed nucleus by inelastic alpha scattering gives rise to a gamma-radiation pattern whose orientation, as the alpha angle is varied, sometimes displays a remarkable reverse rotation determined by the relative phase of the excited rotational states. This arises from the motion of beats occuring where the incoming and outgoing waves overlap at the surface of the nucleus, as has been qualitatively explained in previous communications. The nuclear excitation and subsequent radiation are here discussed somewhat more thoroughly, again in the two-dimensional model, with the aim of exploring the essentials of the mechanism and not hiding them in computation.

IN a strongly absorbing nucleus, a simple surface interaction provides a good approximation and some of the elusive and even questionable features of more complicated reaction calculations are absent. Correspondingly, more striking phenomena sometimes appear and are amenable to simple and direct explanation that should provide a detailed understanding basic to the appreciation of related, more complex phenomena.

When one varies the scattering angle of alphas exciting a $0 \rightarrow 2$ transition in a deformed and strongly absorbing nucleus, the four-lobed angular pattern of the subsequent gammas is sometimes observed[1,2] to rotate rapidly in the reverse direction in a very striking fashion. Some analyses[3] have come close to reproducing this behavior without making very clear the reason for its striking nature. However, it was shown in a preliminary letter[4] that the "beats" of the product of the incoming and outgoing alpha-particle waves, which enter the transition matrix element at the nuclear surface, exhibit just such a reverse rotation in a simple manner; and in a second paper[5] it was shown how the relative phase of the excited 2^+ states is determined by the coincidence in phase of these waves in such a way that the reverse rotation of the "beats" can be passed on to the gamma radiation. Those papers present the main physical idea in a simplified manner and may serve as an introduction to the present treatment which discusses and improves the approximations employed.

MATRIX ELEMENTS

The two-dimensional nucleus was described in Ref. 2 as being deformed from a circular shape, thus

$$r(\psi-\phi)=r_0+r_1\cos\mathfrak{N}(\psi-\phi), \qquad (1)$$

with $\mathfrak{N}=2$ for the usual elliptical deformation. $\mathfrak{N}=3$ describes an octupole, etc. With $\mathfrak{N}=2$, for example, this describes two positive bulges near the major axis (located by ϕ) of the ellipse and negative (inward) bulges near the minor axis. There the analysis was made by integrating properly over ψ. For the sake of physical insight one may further approximate the effect of each of these bulges by a single interaction at the point where the axis intersects the circle, as indicated in Fig. 1. The points on the major axis interact with the scattered particle through a positive δ-function interaction and those on the minor axis, representing a lack of nuclear matter as compared with the circle, through a negative δ function. In order that they may radiate, these points are also endowed with positive and negative electric charges. For a more general deformation with $\mathfrak{N}$ bulges, the interaction with the scattered particle is then represented by a sum over $2\mathfrak{N}$ points:

$$\mathcal{H}'=\sum_{j=0}^{2\mathfrak{N}-1}(-)^j\delta[\mathbf{r}-\mathbf{R}(\phi+2\pi j/\mathfrak{N})], \qquad (2)$$

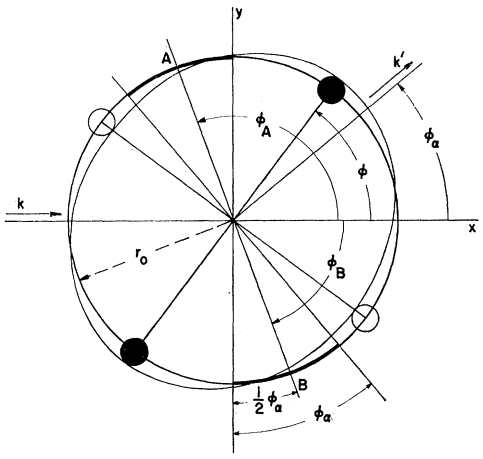

FIG. 1. Discrete points approximating the elliptical distortion in the interaction with the alpha.

* Work performed under the auspices of the U. S. Atomic Energy Commission.

[1] D. K. McDaniels, D. L. Hendrie, R. H. Bassel, and G. R. Satchler, Phys. Letters **1**, 295 (1962); J. G. Cramer, Jr., W. W. Eidson, and D. E. Blatchley, Contributed Papers, Argonne National Laboratory Report ANL-6848, p. 153 (unpublished); J. G. Wills and J. G. Cramer, Jr., *ibid.*, p. 147.

[2] W. W. Eidson, J. G. Cramer, Jr., D. E. Blatchely, and R. D. Bent, Nucl. Phys. **55**, 613 (1964).

[3] E. V. Inopin and S. Shehata, Nucl. Phys. **50**, 317 (1964); J. G. Cramer, Jr., and W. W. Eidson, *ibid.* **55**, 593 (1964).

[4] D. R. Inglis, Phys. Letters **10**, 336 (1964).

[5] D. R. Inglis, in *Preludes in Theoretical Physics in Honor of V. P. Weisskopf*, edited by A. de Shalit, H. Feschbach, and L. van Hove (North-Holland Publishing Company, Amsterdam, 1966).

where $\mathbf{R}(\phi)$ is the position of the interaction point (on the circle at angle ϕ), $\mathbf{r}$ is the position of the scattered particle, and $\mathcal{H}'$ (which should properly contain also a negative strength factor V) is an effective interaction in the distorted-wave Born approximation.

Consider the contribution of the first term $\delta[\mathbf{r}-\mathbf{R}(\phi)]$ to the matrix element $\int d\tau\, \psi_f^* \mathcal{H}' \psi_i$. Here $\psi_f = \xi_f u_f$, for example, the product of an outgoing particle wave $\xi_f(r)$ and an excited nuclear wave function $u_f(\phi)$. In the extreme δ-function approximation, the only relevant values of the particle waves $\xi[R(\phi)]$ are those at the surface and keeping these finite requires that the nucleus be not quite black. The nature of a distorted wave on the surface of an almost black nucleus is suggested by an investigation of Austern[6] which indicates that the phase varies with distance around the edge from about 20° to 150° with very nearly the normal periodicity of the undistorted wave (as pictured in Fig. 4 below). Thus in region A at the top of Fig. 1 (for example), we assume that

$$\xi_i[R(\phi)] = A_i(\phi) \exp[-ikr_0(\phi - \tfrac{1}{2}\pi)]. \tag{3}$$

The amplitude of the product of ξ_i and ξ_f in such a region is expected to decrease as one goes into the shadow region on either side, and this is represented simply by introducing a Gaussian factor for $A_i A_f$ in each of the products:

$$\begin{aligned} P_A &= [\xi_i \xi_f]_A = A_i A_f \exp[-ikr_0(\phi-\phi_A+\tfrac{1}{2}\phi_\alpha)] \\ &\quad \times \exp[ik'r_0(\phi-\phi_A-\tfrac{1}{2}\phi_\alpha)] \\ &= e^{-\frac{1}{2}iS\phi_\alpha} e^{-iD(\phi-\phi_A)} e^{-\beta(\phi-\phi_A)^2}, \\ P_B &= W e^{+\frac{1}{2}iS\phi_\alpha} e^{iD(\phi-\phi_B)} e^{-\beta'(\phi-\phi_B)^2}, \end{aligned} \tag{4}$$

with $S=(k+k')r_0$, $D=(k-k')r_0$, $\phi_A = \frac{1}{2}\pi + \frac{1}{2}\phi_\alpha$ (thus ϕ_A is the middle of the bright sector), and $\phi_B = \phi_A - \pi$. Here W is a weighting factor somewhat less than unity, representing the expectation that the product is somewhat less in and near the shadow sector (region B) than in the bright sector.

The nucleus is treated as a two-dimensional rotor with wave functions $u = e^{im\phi}$. The initial state is the $m=0$ ground state $u_i = 1$, and we let m denote the final-state quantum number: $u_f = u_m = e^{im\phi}$. The integration over the region B then makes the following contribution to the matrix element:

$$\begin{aligned} &\langle m|\mathcal{H}|i\rangle_B \\ &= \int d\phi\, e^{-im\phi} P_B(\phi-\phi_B) \\ &= W e^{i(\frac{1}{2}S\phi_\alpha - m\phi_B)} \int d\phi' \exp[i(D-m)\phi' - \beta'\phi'^2] \\ &= (\pi/B)^{\frac{1}{2}} w_m e^{i(\frac{1}{2}\gamma - m\phi_B)}, \end{aligned} \tag{5}$$

where $\phi' = \phi - \phi_B$, $\gamma = S\phi_\alpha = (k+k')r_0\phi_\alpha$, and

$$w_m = W(\beta/\beta')^{1/2} e^{-(D-m)^2/4\beta'}. \tag{6}$$

Here the integration[7] [which is related to the familiar integral $\int_{-\infty}^{\infty} e^{-\beta x^2} dx = (\pi/\beta)^{1/2}$] is extended between the limits $\pm\infty$ on the presumption that the Gaussian tails cut it off sufficiently rapidly. In the corresponding contribution from region A, the signs of both D and S are reversed, and w_m is replaced by

$$v_m = \exp[-(D+m)^2/4\beta], \tag{7}$$

which lacks the factor W and has β in place of β'.

By lumping a bulge into a point interaction, we have here obtained the same result with a single integration that Ref. 5 derives with a double integration. There the first integration over the distortion of Eq. (1) simply projects out its single Fourier component and selects only the two degenerate excited states $m=\pm 2$. In contrast, a point interaction would be described by an infinite set of Fourier components and there is a matrix element for any m. This single-point treatment is presented here because the two approaches seem to supplement one another in clarifying the nature of the excitation process. The single-point interaction has some similarity to the case of a single orbiting particle.

The sum

$$\langle m|\mathcal{H}|i\rangle = \langle m|\mathcal{H}|i\rangle_A + \langle m|\mathcal{H}|i\rangle_B \tag{8}$$

over the two regions is the matrix element for the case of a single interacting point, with angular coordinate ϕ, on the nuclear surface. If another interacting point, also positive, is added at $\phi+\pi$ (directly opposite the first one), its contribution is calculated from Eq. (5) but with $\phi \to \phi+\pi$. Since the other angles are relative, this appears only in the factor $e^{-im\phi}$ and has the effect of multiplying the matrix element by $e^{im\pi}$. Thus the contribution of the second point just cancels the contribution of the first if m is odd and doubles it if m is even. If the elliptical deformation is approximated more closely by introducing negative δ-function interactions at the positions $\phi+\frac{1}{2}\pi$ and $\phi+\frac{3}{2}\pi$ as represented by the open circles in Fig 1, the total matrix element is again doubled for the cases of greatest interest with $m=\pm 2$ or indeed for any $m=4N+2$, but vanishes if $m=4N$, with N an integer. Thus the coefficients v_m and w_m contain as a common factor the number of interacting points, but only their ratios are important so Eqs. (6) and (7) suffice. With either two or four interacting points, the rotor is invariant to rotation by π and the requirement that the wave function be similarly invariant yields the familiar limitation to states of even m.

NUCLEAR EXCITATION

Perhaps the simplest formulation of scattering theory, although it gives insufficient attention to the question

[6] N. Austern, Ann. Phys. (N. Y.) **15**, 299 (1961). See also I. E. McCarthy and D. L. Pursey, *Proceedings of the International Conference on Nuclear Structure, Kingston, Canada, 1960*, edited by D. A. Bromley and E. W. Vogt (The University of Toronto Press, Toronto, 1960).

[7] D. Bierens de Haan, *Nouvelles tables d'intégrales définies* (Hafner Publishing Company, New York, 1957), p. 262, Eqs. (3) and (4).

of convergence, is the simple time-dependent perturbation theory; and the same discussion of the phases of matrix elements will apply in other formulations. In the present case, one seeks a wave function

$$\psi(t)=u_0\xi_i(r)e^{i\omega_i t}+u_{\rm exc}(\phi)t\xi_f(r)e^{i\omega_f t} \tag{9}$$

with simultaneous excitation of the two degenerate rotational states

$$u_{\rm exc}(\phi)t=\sum_{m=\pm L}a_m(t)u_m(\phi). \tag{10}$$

Here $\xi_i(\mathbf{r})$ is $e^{i\mathbf{k}_i\cdot\mathbf{r}}$ except where it is distorted near the nucleus, and similarly for ξ_f. For small t, $\psi(t)$ is an approximate solution of the time-dependent wave equation containing $\mathcal{H}_0+\mathcal{H}'$ if

$$\dot{a}_m(t)=\langle u_m\xi_f|\mathcal{H}'|u_0\xi_i\rangle e^{i(\omega_i-\omega_f)t}.$$

For those values of k_f within the narrowing band[8] satisfying the relation $(\omega_f-\omega_i)t\ll\frac{1}{2}\pi$, the associated excitation of the nucleus is described by

$$\begin{aligned}u_{\rm exc}(\phi)&=\sum_{m=\pm L}\langle m|\mathcal{H}'|i\rangle e^{im\phi}=\sum_{m=\pm L}\langle e^{-im\phi}\xi_f(r)|\mathcal{H}'|\xi_i(r)\rangle e^{im\phi}\\&=(\pi/\beta)^{1/2}\sum_{m=\pm L}(v_m e^{-i\gamma/2}+w_m e^{i\gamma/2})e^{im(\phi-\phi_B)}\\&=(\pi/\beta)^{1/2}e^{-i\gamma/2}\sum_{m=\pm L}(v_m+w_m e^{i\gamma})e^{im\phi'},\end{aligned} \tag{11}$$

with $\phi'=\phi-\phi_B$. Here we have made use of Eqs. (5)–(8). The orientation of the gamma pattern will be seen to depend on the relative phase of the two terms $m=\pm L$. To formulate this, set

$$v_m+w_m e^{i\gamma}=C_m e^{i\delta_m}, \tag{12}$$
$$C_m=\{v_m{}^2+2v_m w_m\cos\gamma+w_m{}^2\}^{1/2}.\quad\text{(positive)}$$

We then have

$$u_{\rm exc}=(\pi/\beta)^{1/2}e^{i(\gamma+\delta_L+\delta_{-L})/2}\times\{C_L e^{iL(\phi'-\phi_0')}+C_{-L}e^{-iL(\phi'-\phi_0')}\}, \tag{13}$$

with

$$\phi_0'=\phi_0-\phi_B=(1/2L)(\delta_{-L}-\delta_L).$$

This phase angle ϕ_0' may be determined by use of Eq. (12) with $m=L$ and $-L$:

$$e^{i(\delta_L-\delta_{-L})}=e^{i2L\phi_0'}=(v_L+w_L e^{i\gamma})\times(v_{-L}+w_{-L}e^{-i\gamma})/C_L C_{-L}. \tag{14}$$

Hence,

$$\frac{\sin 2L\phi_0'}{\cos 2L\phi_0'}=\frac{(v_{-L}w_L-v_L w_{-L})\sin\gamma}{v_L v_{-L}+w_L w_{-L}+(v_{-L}w_L+v_L w_{-L})\cos\gamma}, \tag{15}$$

$$\phi_0=\phi_B-\frac{1}{2L}\tan^{-1}\left(\frac{q\sin\gamma}{p+\cos\gamma}\right), \tag{16}$$

with

$$p=S_0/S_+,\qquad q=S_-/S_+, \tag{17}$$
$$S_0=v_L v_{-L}+w_L w_{-L},\quad S_\pm=v_{-L}w_L\pm v_L w_{-L}.$$

Thus the result has the same simple form[9] as has Eq. (17) of Ref. 2, although the latter was derived (with $L=2$) a little more simply by setting $w_{-2}=0$ from the outset. As was there remarked, v_{-L} and w_L, having $(D-L)^2$ in the negative exponent of Eqs. (6) and (7), are larger than v_L and w_{-L}, respectively, which have $(D+L)^2$ in the exponent. This is a remnant of the conservation of momentum as the particle loses forward momentum to the nuclear excitation locally in region A or B. The smallest of the four is w_{-L} because it also contains the factor $W(\beta/\beta')^{1/2}<1$.

The similarity between the previous result and this result which takes w_{-L} into account means that the mechanism illustrated in Fig. 6 of Ref. 5 is also applicable for the solution of Eq. (16). That is, ϕ_0 either varies in a narrow range or continues to increase and exhibits the reverse rotation, depending on whether p is greater than unity. The factor q makes curve D for the $\tan^{-1}$ have a smaller slope than curve C where they cross zero together, thus tending to make curve D more S-shaped. While available observations apply to $L=2$, one sees that similar results are in principle possible with $L=3$ or $L=4$ if the nucleus has an appropriate deformation.

The shape of the curve for ϕ_0 in Eq. (16) is more sensitively dependent on the value of the parameter p, as is illustrated for $L=2$ by the curves for four values of p in Fig. 2, each of these curves being similar to Fig. 6 of Ref. 5. Since q is expected to be somewhat less than unity, q is taken to be 0.9 in all these graphs. As p increases towards unity, the curve for $A=p+\cos\gamma$ becomes zero at points farther out towards the edge of the region plotted, so that the range in which the arctangent varies from $-\frac{1}{2}\pi$ to $\frac{1}{2}\pi$ is forced further out towards the edges and hence this function becomes steeper near the edges, leaving it flatter near the middle. When p becomes greater than unity, A is nowhere zero so the tangent is never infinite and the arctangent remains between $-\frac{1}{2}\pi$ and $\frac{1}{2}\pi$, with no secular increase.

THE RADIATION PATTERN

From Eq. (13), the probability distribution of the nuclear axis ϕ is given by

$$\begin{aligned}u_{\rm exc}u_{\rm exc}{}^*&\propto C_L{}^2+C_{-L}{}^2+C_L C_{-L}[e^{i2L(\phi-\phi_0)}+e^{-i2L(\phi-\phi_0)}]\\&=\sigma_\alpha+2C_L C_{-L}[1-2\sin^2L(\phi-\phi_0)]\\&=A'-B\sin^2L(\phi-\phi_0),\end{aligned} \tag{18}$$

[8] L. I. Schiff, *Quantum Mechanics* (McGraw-Hill Book Company, Inc., New York, 1949), Fig. 27.

[9] *Note added in proof.* This form has been obtained also by B. J. Verhaar and L. D. Tolsma, Phys. Letters **17**, 53 (1965). In place of the gradual Gaussian termination used here to evaluate v_m and w_m, these authors introduce a sharp (but symmetric) cutoff. To derive this form it is indeed not necessary to evaluate v_m and w_m explicitly, but merely to make them real by weighting each integration symmetrically about its midpoint. The relative magnitudes may then be surmised qualitatively from the remark about vestigial conservation of local momentum.

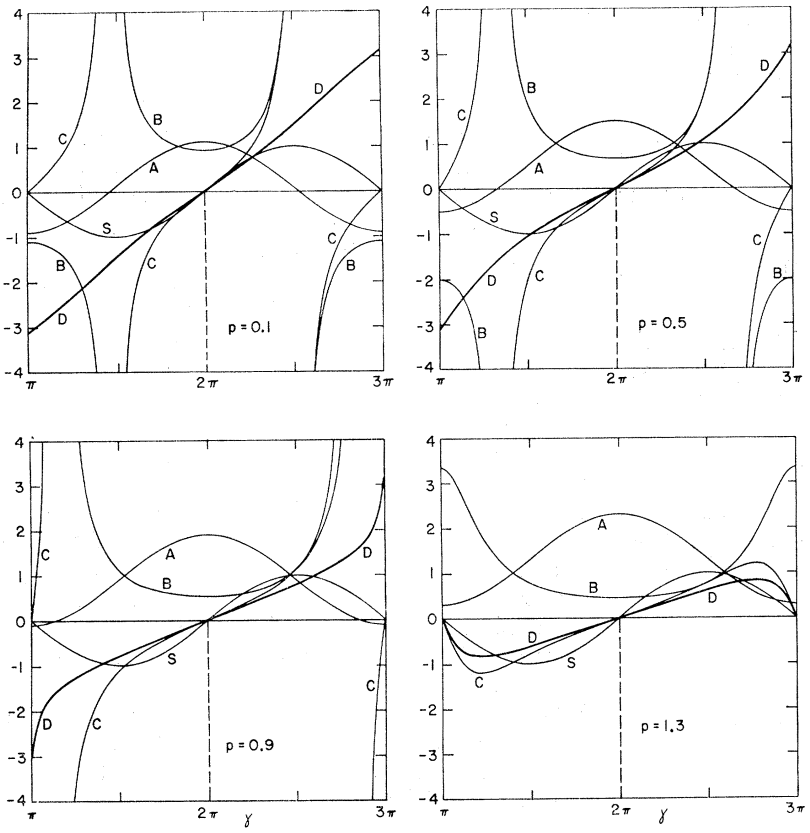

FIG. 2. Determination of the shape of the reverse rotation curve by the factors of Eq. (16) for several values of p. The curve labels are as follows: $S=\sin\gamma$. A is the denominator, $A=p+\cos\gamma$. B is its reciprocal and passes through infinity successively in opposite directions, $B=1/A$. C is obtained by multiplying B and S, and passes through infinity always in the same direction (except when $p>1$ as in the last graph). $D=\tan^{-1}C$ and continually increases. It is plotted modulo 2π, so as to keep it between $-\pi$ and π, corresponding to the way the experimental points are plotted in Ref. 2 and Fig. 6.

in which A' and B are positive and

$$\sigma_a=C_L{}^2+C_{-L}{}^2=\sum_{m=\pm L}(v_m{}^2+w_m{}^2+2v_mw_m\cos\gamma). \quad (19)$$

The symmetry of the pattern of emitted γ radiation is,

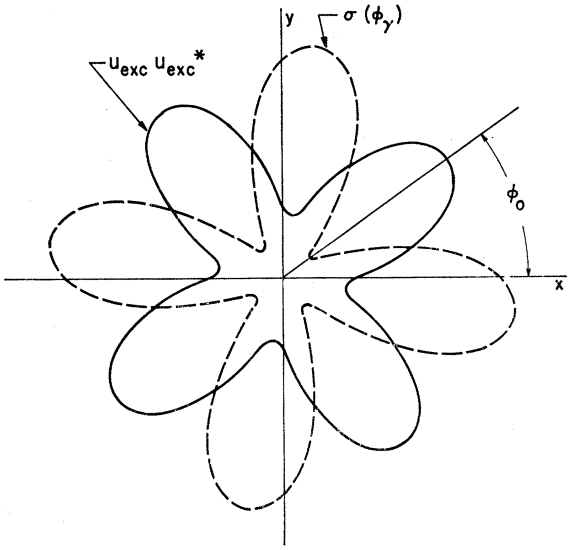

FIG. 3. The phase of the angular pattern of the gamma radiation relative to the probability distribution of the major axis of the elliptical nucleus in the excited state $L=2$.

of course, determined by the symmetry of the charge distribution; but there remains the question of a possible phase difference between the two patterns. This is determined semiclassically by the fact that a varying current element radiates preponderantly in a direction normal to itself. The energy flux[10] radiated in the direction of the wave vector $\boldsymbol{\kappa}$ is proportional to the square of the matrix element of the product $e^{i\boldsymbol{\kappa}\cdot\mathbf{r}}$ multiplied by the component of the gradient normal to $\boldsymbol{\kappa}$. That is,

$$\sigma(\phi_\gamma)\propto\left|\int d\tau\, u_0{}^*e^{i\boldsymbol{\kappa}\cdot\mathbf{r}}\nabla_{\perp\kappa}u_{\rm exc}\right|^2. \quad (20)$$

For a charge at a point $\mathbf{R}(\phi)$ moving around a circle (as do the points representing bulges on the surface of the deformed nucleus) the normal component of the gradient operator is

$$\nabla_{\perp\kappa}=R^{-1}\cos(\phi-\phi_\gamma)(\partial/\partial\phi), \quad (21)$$

where ϕ_γ gives the direction $\boldsymbol{\kappa}$ in which the γ radiation is observed. The various multipole orders of the radiation correspond to terms in the expansion

$$e^{i\boldsymbol{\kappa}\cdot\mathbf{r}}=\textstyle\sum_n(i\boldsymbol{\kappa}\cdot\mathbf{r})^n/n!=\sum_n[i\kappa r\cos(\phi-\phi_\gamma)]^n/n!, \quad (22)$$

in which $n=0$ gives the dipole term, $n=1$ the quadrupole, etc. With $u_{\rm exc}$ given by Eq. (13), the matrix ele-

[10] Reference 8, Sec. 36.

ment thus contains integrals of the type

$$\int d\phi \cos^{n+1}(\phi-\phi_\gamma)\frac{\partial}{\partial\phi}u_{\rm exc}(\phi)$$
$$= iL\int d\phi[e^{i(\phi-\phi_\gamma)}+e^{-i(\phi-\phi_\gamma)}]^{n+1}$$
$$\times[C_L e^{iL(\phi-\phi_0)}-C_{-L}e^{-iL(\phi-\phi_0)}]$$
$$= 2\pi iL\{C_L e^{iL(\phi_\gamma-\phi_0)}-C_{-L}e^{-iL(\phi_\gamma-\phi_0)}\}$$
$$\text{with}\quad n+1=L. \quad (23)$$

With $n+1\neq L$ the integral vanishes, since only in the case of the two end terms of the binomial expansion with $n+1=L$ does the product of the exponentials equal unity. The radiation pattern is then given by the absolute square of this amplitude; that is,

$$\sigma(\phi_\gamma)\propto C_L{}^2+C_{-L}{}^2-2C_LC_{-L}\cos 2L(\phi_\gamma-\phi_0)$$
$$= A+B\sin^2 L(\phi_\gamma-\phi_0), \quad (24)$$

where $B=4C_LC_{-L}$ is the same as in Eq. (18) and $A=(C_L-C_{-L})^2=A'-4C_LC_{-L}$ is less than A' but still positive. Thus the radiation pattern has a greater maximum/minimum ratio than has the probability distribution. The differentiation in Eq. (23) changes the sign of the term in C_{-L} and thus of the term in B, so the radiation pattern in Eq. (24) has its maxima and minima interchanged from those of the probability distribution of the nuclear symmetry axis, Eq. (18), as is very familiar in the case of dipole radiation ($L=1$) with the radiation normal to the dipole distribution. The phase relation between the two patterns for $L=2$ is shown in Fig. 3.

OPTICAL-MODEL WAVE FUNCTIONS

While Fig. 2 gives ϕ_0 as a function of γ for given p and q, it is desirable for the sake of comparison with experiment to display it as a function of ϕ_α with p and q also functions of ϕ_α for some reasonably simple treatment of the wave functions. Austern's treatment, already mentioned, of an almost black three-dimensional nucleus, however, suggests features that may be essential. His results (from his Fig. 5) are given by the broken lines in Fig. 4 and are approximated by the solid straight-line segments that simplify the description. As a reasonable basis for an exploratory two-dimensional calculation, we assume accordingly that the distorted wave ξ_i or ξ_f at the surface has constant phase within $\frac{1}{8}\pi$ of the axis of the wave on the "bright" side, and that beyond this the phase varies linearly around the surface with the wave number k or k' that it has in free space.

These regions of constant phase, represented by the short horizontal segment from $157\frac{1}{2}°$ to 180° in Fig. 4, of either ξ_i or ξ_f are indicated by the cross-hatched regions in Fig. 5. In this figure, the regions A and B are characterized by a product wave $\xi_i\xi_f$ with the small

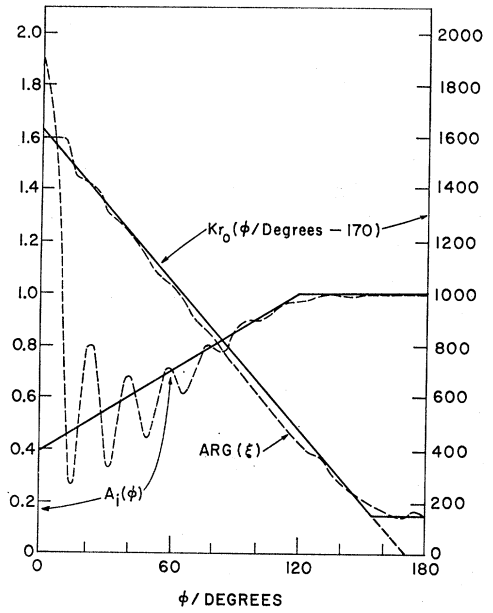

FIG. 4. Variation of the amplitude and phase of a wave incident on an almost-black nucleus as suggested by Austern (broken lines) and as here approximated by straight lines.

wave number $k'-k$, as envisaged in the integrations (5) yielding v_m and w_m. Here the substantial contributions to the integral arise from the slow variation of phase. In the cross-hatched regions the wave number is k or k'; and in the adjacent regions, between these and the edges of region B, the wave number has the even larger value $k+k'$. In these regions the variation of phase is so rapid that the contributions are small and may be neglected. In order to suppress these contributions and still leave the simplicity of the Gaussian form in P_A and

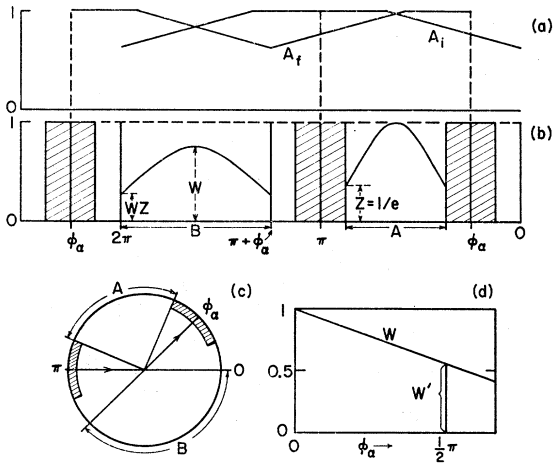

FIG. 5. (a) The overlap of the shadow amplitudes, idealized from Fig. 4, at various angles. (b) The cross-hatched regions where the contribution is small [shown also in (c)] and the Gaussian approximations to the product A_iA_f. (d) The linear dependence assumed for the factor expressing the weakness of the shadow region.

P_B, we determine β and β' in Eq. (4) to make these amplitudes in A and B reduce at the edges of these regions to a fraction Z of their maxima as indicated in Fig. 5(b) with $Z=1/e$. Thus, $\beta=-4(\ln Z)/(\phi_\alpha-\frac{3}{4}\pi)^2$, and $\beta'=-4(\ln Z)/(\phi_\alpha-\pi)^2$ is somewhat smaller since region B is somewhat wider than region A.

In Fig. 5(a), the amplitude A_i is represented by a line extending horizontally out to 60° on either side of π and then sloping gently beyond, as suggested by the simplification introduced in Fig. 4, and the diagram for A_f is similar. While the Gaussian in region B is a poor fit to the product A_iA_f because of the need to cut off at the edge of the region, the factor W (the amplitude at the center of the region relative to that in region A) should be determined by this product at the center of the region (or by a corresponding matching of integrals). For the case drawn in Fig. 5(a), for example, this product is very nearly unity (0.96) in the middle of region A and is about 0.75 in the middle of region B, so that $W\approx 0.75/0.96=0.78$. It is clear that W thus starts at unity where $\phi_\alpha=0$ and decreases steadily with increasing ϕ_α. We approximate this situation by assuming a linear decrease of W [as shown in Fig. 5(d)] from unity at $\phi_\alpha=0$ to W' at $\phi_\alpha=\frac{1}{2}\pi$ and beyond, and we treat W' as a parameter describing this shadow effect.

In exploring the general features that may give rise to the observed rotation of the gamma-ray pattern, it is of interest to determine to what extent such a simplified description of the black-nucleus wave functions may account for the observations. The simplifications make it possible to give analytic expressions for β, β', and W that may be used to determine how ϕ_α specifies the quantities p and q which govern the shape of the curves of ϕ_0 in the way shown in Fig. 2 and the accompanying discussion. The experimental example selected for comparison is Mg^{24} and the wave numbers k and k' employed are those for this case. (The results are not very sensitive to small changes in these.) We thus take $E_{\text{lab}}=22.5$ MeV, $E_{\text{c.m.}}=(6/7)E_{\text{lab}}=19.28$ MeV$=37.7\ mc^2$, so that

$$k=(2\mu E_{\text{c.m.}})^{1/2}=[2(24/7)37.7]^{1/2}\times(1840^{1/2}/137)mc^2/e^2=5.03\ mc^2/e^2;$$
$$k'/k=[(19.28-1.37)/19.28]^{1/2}=0.9638$$

(the excitation energy of the $L=2$ state being 1.37 MeV); and $(k+k')/k=1.964$, $(k-k')/k=0.362$.

In order to avoid arbitrary parameters wherever possible, r_0 should ideally be determined from the elastic scattering and then used in the calculation of the gamma orientation. While very useful for the sake of a qualitative understanding, however, the two-dimensional diffraction does not give a quantitative fit to the scattering data and thus leaves some latitude in the appropriate choice of r_0. The elastic scattering shows minima at 39°, 57°, 77°, and 99° for $N=2$, 3, 4, and 5, respectively, from which the simple two-dimensional diffraction formula $2kr_0\sin\frac{1}{2}\phi_\alpha=\pi N$ yields $r_0/(e^2/mc^2)=1.87$, 1.96, 2.10, and 2.05, respectively, with appreciable variation. A modified formula treating the nucleus as a black circle in two dimensions, $r_0=2\pi N/k(\phi_\alpha+2\sin\frac{1}{2}\phi_\alpha)$ yields instead 1.83, 1.90, 1.91, and 1.90 with less variation. The corresponding values for the three-dimensional diffraction model, obtained by setting $J_1(2kr_0\sin\frac{1}{2}\phi_\alpha)=0$, are 2.08, 2.11, 2.12, and 2.14, with still less variation. These values are somewhat larger than for two dimensions because the contribution to diffraction from near the extremities of $\mathbf{K}\cdot\mathbf{r}$ are less important for a circle than for a line or rectangle. These radii in three dimensions may be interpreted as distances of contact of two spheres, $(24^{1/3}+4^{1/3})a_0$, with $a_0=1.33$ F$=0.47e^2/mc^2$ which is about the usually accepted figure. The value of r_0 employed in the following, $r_0=1.83e^2/mc^2$, is consistent with the latitude suggested by the two-dimensional fit to the scattering, but is chosen a few percent on the low side of the suggested value $1.9\ e^2/mc^2$ to improve slightly the fit to the gamma-ray data. The consequent values $S=5.03\times1.83\times1.964=18.1$ and $D=5.03\times1.83\times0.0362=0.333$ are used in the equations [(6) and (7)] for γ, v_m, and w_m, along with the values of β and β' determined as functions of ϕ_α by the arbitrary parameters Z and W'. The values of v_m and w_m and the subsequent quantities $S_\pm$, S_0, p, and q of Eq. (17) are plotted as functions of ϕ_α in Fig. 6, for the typical parameters $Z=1/e$ and $W'=0.8$. It is seen

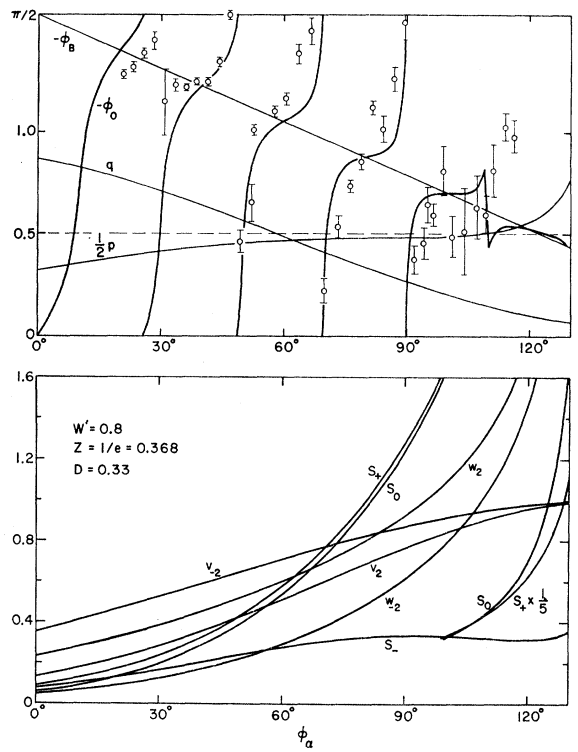

FIG. 6. The experimental results showing the reverse rotation for Mg^{24} at $E_\alpha=22.5$ MeV, from Ref. 2, as compared with theoretical curves for favorable values of the parameters. The variation of some of the subsidiary functions is also shown.

that at larger angles ϕ_α, with the narrowing ranges of integration A and B, there is only a slight tendency for conservation of angular momentum and that w_{-2} is no longer negligibly small (as it was assumed to be in Ref. 5), so that q is appreciably less than unity.

These values of the parameters in Eq. (16) determine the variation of the gamma orientation angle ϕ_0 which is plotted in the same figure. As is consistent with Fig. 2, the curve continues to go out of the top and return from the bottom of the figure only as long as $p<1$; and near the successive points where the curve crosses the line ϕ_B it becomes flatter as p approaches 1. In Fig. 2, the parameter q was taken to be 0.9, and in Fig. 6 the decreasing q at the larger values of ϕ_α further flattens the curve for ϕ_0 as it crosses ϕ_B, as is clear from the construction of Fig. 2.

COMPARISON WITH EXPERIMENT

The experimental points the Indiana group obtained for Mg^{24} at $E_\alpha=22.5$ MeV are also shown in Fig. 6. It is seen that the theory qualitatively reproduces the two striking sweeps from the bottom to the top of the graph between 50° and 90°—one example of the phenomenon this study was designed to elucidate. However, in consequence of choosing the parameters to make this rapid reverse rotation cease for $\phi_\alpha>90°$ (as suggested by the experimental points there), the theoretical curves are much more S-shaped (flatter near ϕ_B) than the experimental ones. The principal discrepancy is at forward angles: The formulation of the theory provides no clue as to why the reverse rotation is lacking there while it exists in the range 50° to 90°.

DISCUSSION OF PARAMETERS

A mathematician is quoted as saying, "If you give me two parameters, I will describe an elephant. If you give me a third parameter I will make him wiggle his trunk." In this simplified formulation of the gamma-rotation problem, we have left the two parameters Z and W' completely free and have made a slight adjustment of a third r_0 and have achieved only partial agreement with the salient feature. Both here and in the consideration of other experiments it is of interest to investigate the sensitivity of the results to variation of the parameters.

The value $r_0/(e^2/mc^2)=1.83$ was chosen by adjusting it downward slightly to make the curve for ϕ_0 pass out of the top of the graph at 90°, where there is an experimental point; with the original value 1.9 taken directly from scattering, it goes off at 85°.

The value $W'=0.8$ is higher than would be expected from the treatment of Figs. 4 and 5 or from off-hand judgement of the intensity on the shaded side of an opaque nucleus. The linearization of the amplitude of the wave function for three dimensions in Fig. 4 suggests a lower limit of 0.4 at 0°. In Fig. 5(a) this has been raised to 0.7 for two dimensions, and even this higher value suggests $W'=0.56$ [so as to make $W(45°)=0.78$].

The influence of altering W', Z, and (for the sake of experiments on other nuclei) D is shown in the examples of Fig. 7. Reducing W' keeps region B from competing strongly enough with region A to give the reverse rotation at large ϕ_α. Increasing Z broadens the regions A and B but has rather little effect. Increasing D increases the discrimination between momentum transfers—thus decreasing w_{-2}, increasing q and making ϕ_0 a little less flat where it crosses ϕ_B.

Thus, in order to make the "elephant's trunk wiggle" at large enough angles, we have had to increase the contribution from the shadowed side of the nucleus by means of an artifically large W'. It may be that in actual nuclei this region does contribute more than our black-nucleus model would suggest because actual nuclei are not completely opaque and transmission through the edge of the nucleus permits a higher intensity to reach this region. A differential of this effect, a cutoff of this penetration as ϕ_α becomes larger than about 90°, might account for a rapid change, between 80° and 100°, of the flatness of the curve for ϕ_0 where it crosses ϕ_B. But our inability to get rid of the wiggle at forward angles while preserving it at moderate angles reminds us that the model does not take into account all possible effects. In particular, the irregular change of phase near the "focus" at 0° in Fig. 4 (or of an even more intense focus in a partially transparent nucleus) and the effect this may have as it approaches the cross-hatched region of calm of the other wave in Fig. 5, may have a profound influence at forward angles but appears to be somewhat more awkward to formulate analytically than the effects that have been approximated in this discussion.

Perhaps the most questionable feature of the model is thus the sharp edge of the completely absorbing nucleus. An interference pattern is so general a phenomenon that use of optical-model codes for the interpretation of forward alpha scattering characteristically yields several acceptable sets of optical-model parameters. In an interpretation of the reverse rotation of the γ-ray pattern by means of the DWBA (distorted-wave Born approximation), Eidson *et al.*[11] find that one out of about six such sets of parameters also reproduces the dramatic cycles about as in Fig. 6. (The other choices of parameters give practically no reverse rotation at all.) With so much choice having been exercised, it is not clear whether the agreement is real or fortuitous. The fact that the potential is shallow (20 MeV real) is not disturbing since it should in some sense represent an attraction between alphas within which nucleon forces are already largely saturated. The fact that it is rather transparent to alphas (3 MeV imaginary) departs markedly from the simple concept that a black nucleus

[11] W. W. Eidson (private communication).

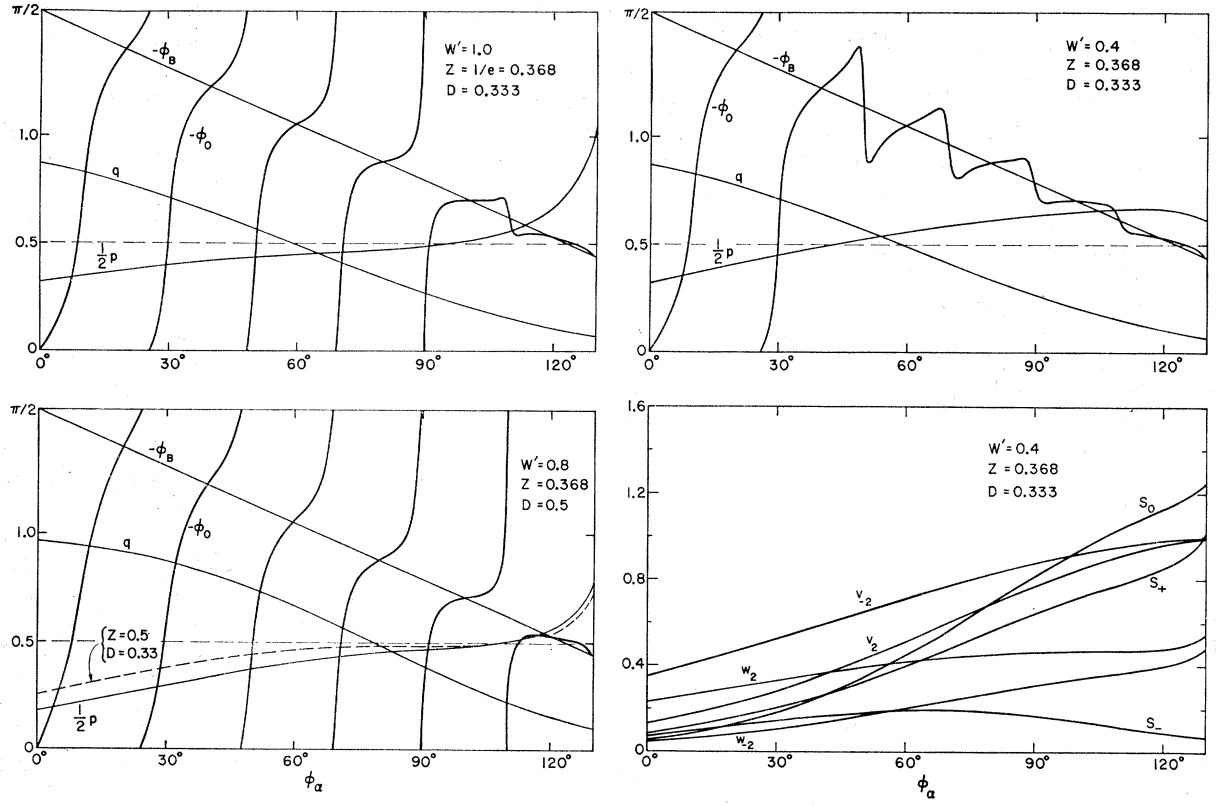

FIG. 7. Examples to illustrate how the shape of the curves for orientation of the gamma pattern depends on the parameters.

is responsible for the elastic-inelastic phase rule, but may correspond to reality.

If our simple model is indeed at fault in being too sharply opaque, it still aptly illustrates how in principle the reverse motion of the beats of the external waves can be responsible for a rapid reverse rotation of the γ-ray pattern. It also helps one appreciate that the phase determination is rather fragile so that the reverse rotation may appear in one experimental circumstance and not in another.

ACKNOWLEDGMENTS

Thanks are due to Professors J. G. Cramer, W. W. Eidson, and J. G. Wills of Indiana University for informative discussions of their very interesting results, and to Dr. Stanley Cohen for use of a code for the preparation of graphs. I wish also to thank Professor R. Bouchez and his colleagues at l'Université de Grenoble for their hospitality and interest during a stay there while this work was in progress.